Accepted Manuscript

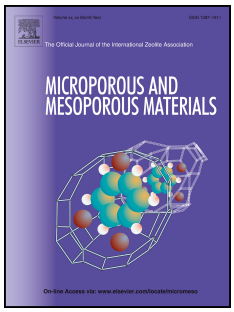

Tunable interlayer hydrophobicity in a nanostructured high charge organo-mica

Carmen Pesquera, Fernando Aguado, Fernando González, Carmen Blanco, Lidia Rodríguez, Ana C. Perdigón

PII: S1387-1811(17)30787-4

DOI: 10.1016/j.micromeso.2017.12.006

Reference: MICMAT 8695

To appear in: *Microporous and Mesoporous Materials*

Received Date: 23 October 2017

Revised Date: 5 December 2017

Accepted Date: 8 December 2017

Please cite this article as: C. Pesquera, F. Aguado, F. González, C. Blanco, L. Rodríguez, A.C. Perdigón, Tunable interlayer hydrophobicity in a nanostructured high charge organo-mica, *Microporous and Mesoporous Materials* (2018), doi: 10.1016/j.micromeso.2017.12.006.

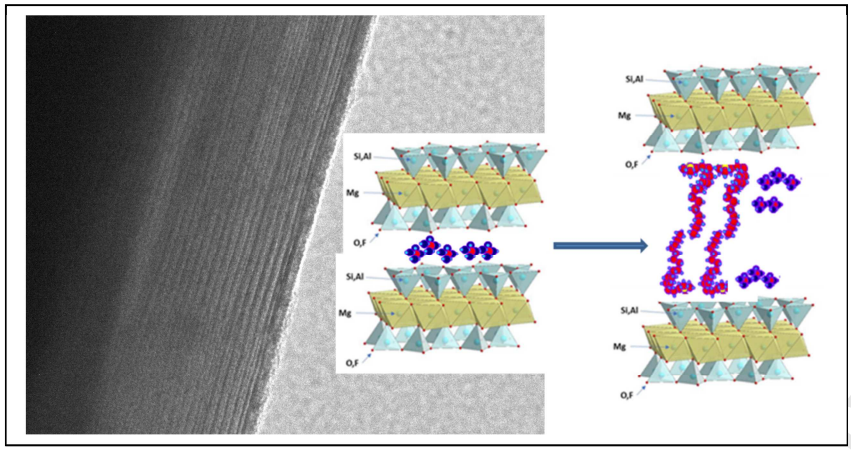

Tunable interlayer hydrophobicity in a nanostructured high charge organo-mica

Carmen Pesquera,[†] *Fernando Aguado*[‡] *, Fernando González*[†]*, Carmen Blanco*[†]*, Lidia Rodríguez*[§] *and Ana C. Perdigón*[*,†]

[†] Departamento de Química e Ingeniería de Procesos y Recursos, Escuela Técnica Superior de Ingenieros Industriales y de Telecomunicación, Universidad de Cantabria, Avda. de Los Castros s/n, 39005, Santander, Spain. [‡] Departamento de Ciencias de la Tierra y Física de la Materia Condensada, Facultad de Ciencias, Avda. de Los Castros s/n, 39005, Santander, Spain. [§] Servicio de Caracterización de Materiales (SERCAMAT), Universidad de Cantabria, Plaza de la Ciencia s/n, 39005, Santander, Spain

A tunable hydrophobicity, from a fully hydrophobic medium to an amphiphilic quasi-solution, has been obtained in the interlayer space of a synthetic high charged mica by ion exchange reaction with amine cations. The structural and intercalation properties of the hybrids after the exchange with the n-alkylammonium cations: $[RNH_3]^+$, $[RNH(CH_3)_2]^+$ and $[RN(CH_3]_3^+$ with C16 alkyl chain length have been determined by termogravimetric/differential scanning calorimetry analysis (TGA-DSC) and mass spectrometry (MS), X-ray diffraction (XRD) and Fourier transform infrared spectroscopy (FTIR). Transmission electron microscopy (TEM) has been used as a complementary technique to provide new insights into the morphology of the exchanged products. Coverage and cation distribution have been correlated with layer charge and

steric effects. Thus, a full organo-clay is obtained when the primary amine cations are adsorbed between the layers. However, a homogenous single phase of mixed organic/inorganic cations is formed in the same interlayer with the tertiary amine cations. Mixed ion clays combining both exchangeable inorganic and adsorbent organic ions in their interlayer space can be potential materials to be used as adsorbents for water decontamination, independently of the hydrophilic/ hydrophobic nature of the pollutants. For the quaternary amine cations steric effects preclude the coexistence of both organic and inorganic species in the same interlayer of the clay so phase segregation together with a heterogeneous phase of organic and inorganic galleries in the same particle can be observed.

1. Introduction

Synthetic high charge mica-type aluminosilicates have attracted the interest of the scientific community because of their distinctive exchange properties.[1] They have a theoretical cation exchange capacity (CEC) of up to 468 meq 100 g^{-1}, whereas other swelling low charge clays have typical values from 80 meq 100g^{-1} (Wyoming montmorillonite) to 170 meq 100g^{-1} (saponite). Also, they have shown preferential selectivity for harmful divalent and heavy metal cations;[2, 3, 4] hence they have been proposed as efficient adsorbents for removal of pollutants from water and for capture and immobilization of radioactive waste.[5, 6] High charge mica-type clays have a 2:1 layered structure with a high negative charge density from isomorphous substitution of aluminum for silicon in the tetrahedral sheet. Unlike natural micas, the layer charge is balanced by exchangeable sodium cations, up to four per unit cell (uc), located in the interlayer space of the aluminosilicate.[7] In this way, cation exchange properties of a set of hydrated monovalent and divalent metal ions on an ultrafine Na-4-Mica have been already characterized. In every case the extension of the cation exchange was below half of the theoretical exchange capacity associated to these samples, -around 200meq 100g^{-1} of clay-.[8] This behavior has been related to the difficulty of the cations to diffuse in the narrow interlayer space or to the fact that clay edges could collapse at the beginning of the process, preventing the exchange to proceed. In any case, because of the limited exchange capacity, the diffusion of cations through the interlayer space of Na-n-Micas could generate a heteroionic structure, still not identified.

Also the intercalation properties of layered clay minerals have allowed the synthesis of new materials with important applications. For instance, voluminous inorganic polycations are incorporated in the interlayer space and polymerized creating porous derivatives useful in

catalysis.[9] It has been established that ion exchange is strongly influenced by the size of the complex in the aqueous solution, being less effective as the hydrated ionic radius increases. Many of these synthesis strategies require a surfactant templating approach to direct the polymerization of the inorganic wall. It is well known that the incorporation of long alkyl chain length surfactants between the layers of low charge aluminosilicates results in ordered organic–inorganic nanocomposite material wich combines the functionality of an organic molecule or polymer, with the structural properties of the inorganic component.[10] In particular, adsorption of surfactant cations distributed in the interlayer space of the clay, creates the optimal level of hydrophobicity required for different industrial uses in many areas, from porous solids precursors with application in catalysis, for oil industry where the permeability and stability properties of drilling fluids are mainly controlled by polymer-clay nanocomposites, or as adsorbents for removal of organic waste.[11] In particular, high charge micas have shown their ability as precursor of novel mesoporous materials with enhanced acidity, through a surfactant templating strategy. [12] The porous formation is driven by the exclusive use of long quaternary amine~~s~~ cations as a template, with two fundamental purposes: (1) to improve the accessibility to the bidimensional galleries of the aluminosilicate and (2) to direct the polymerization of the silica source. A deeper knowledge of the intercalation chemistry is desirable to control the adequate level of hydrophobicity required for each application. In that context, the hydrophobic properties of the intercalated compounds are governed by the equilibrium of several forces: (1) the electrostatic interaction between the clay surface and the head group of the surfactant and (2) the Van der Waals interaction between tails; and also governed by steric constriction (chain length effect and head group size effect). This delicate equilibrium between forces may lead to the formation of different exchanged products as a function of coverage. Phase segregation of the

organo-clay and the inorganic-clay can occur when the exchange capacity of the silicate is not fully satisfied. Also an homogeneous single phase of mixed organic and inorganic cations in the interlayer space compensating the layer charge can be formed; or even a heterogeneous phase of alternating organic and inorganic galleries. Pinnavaia et al. elucidated the formation processes for a heterostructure containing regularly alternating interlayers of sodium and alkylammonium cations from a fluorohectorite, in which both the length of the alkyl chain in terms of hydrophobic interactions and the size of the surfactant head group play a role.[13] A recent Monte Carlo simulation study of the adsorption of alkyltrimethylammonium chloride on a Wyoming-type montmorillonite suggests that even at the highest coverage, a fraction of Na^+ ions remains adsorbed above the tetrahedral substitutions of the clay surface in a homogeneous single phase, the excess of positive charge being compensated by chloride counter-anions.[14] Klapyta *et al.* identified polyphase systems with various arrangements of the organic species (monolayer, bilayer and pseudotrilayer), when n-alkyltrimethylammonium cations with alkyl chain lengths of C12 and C18 are fully adsorbed on two synthetic micas, probably as a consequence of the heterogeneous layer charge distribution.[15] Also, regular alternating organic heterostructure is formed when the naturally occurring 2:1 silicate rectorite is exchanged with $C_{16}H_{33}PBu_3^+$. Rectorite is a rarely interstratified silicate of high charge non-swellable mica-type galleries and low charge swellable smectite-type galleries.[16]

Few investigations have been conducted on the intercalation chemistry of high charge micas with long alkylammonium cations and none has been focused on the exchanged hybrid material when the interlayer cation is not fully replaced by the organic matter. Alba *et al*. have described the formation of a homogenous single-phase organic-clay upon intercalation of the highly charge synthetic mica with primary n-alkylammonium cations of varying alkyl chains lengths, from C12

to C18. The primary amine cations in the interlayer were closely packed in a paraffin-type bilayer with double all-trans conformation due to the high density of the organic matter.[17, 18, 19] We present in this work a deep insight into the intercalation properties of a swellable high charge mica Na-4-Mica, with a primary $[RNH_3]^+$, tertiary $[RNH(CH_3)_2]^+$, and quaternary amine cations $[RN(CH_3)_3]^+$, with alkyl length R = 16. The length of the surfactant cations has been carefully chosen to assure that Van der Waals interactions between alkyl chains are strong enough to allow a quantitative uptake of the surfactant cations. The role of the surfactant head groups, in terms of size and hydrophilicity, on the formation of the heteroionic structures, when the exchange capacity is not fully satisfied, has been also determined. Special attention has been paid to understand the composition of the interlayer space as a function of the amphiphilic surfactant nature. The organic-inorganic hybrid structure of the product has been analyzed using X-ray diffraction, taking into account geometrical considerations. Transmission electron microscopy, thermogravimetric analysis combined with mass spectroscopy and Fourier transform infrared spectroscopy have provided valuable information about the distribution and packing properties of the organics, helping to identify the exchanged products. In the present study a correlation between coverage and intercalation properties of high charge micas has been established in terms of layer charge and surfactants' nature. Thus, a tunable hydrophobicity in the interlayer space of the hybrid material can be obtained under particular experimental conditions, from a fully hydrophobic medium to an amphiphilic quasi-solution, valuable for several material applications. Mixed ion clays that combine both exchangeable inorganic and organic ions in their interlayer space can be potential materials to be used as adsorbents for water decontamination, independently of the hydrophilic or hydrophobic nature of the pollutants.

2. Experimental

2.1. Synthesis of high charge micas.

Na-4-Mica, with four negative charges per unit cell in its structure, was synthesized following the "NaCl method" described by Park et al.[20] Stoichiometric amounts of SiO_2, (from Sigma, purity 99.8 %), $Al(OH)_3$ (from Riedel-de-Haën, purity 99.7 %), MgF_2 (from Aldrich, purity 99.9 %), and twofold the stoichiometric amount of NaCl (from Panreac, purity 99.9 %) were well mixed in an agate mortar. Reactants were thermally treated in a Pt crucible at 900 °C for 15 h and leave to cool down. After cooling, the solid was washed with deionized water to eliminate the excess of NaCl and dried at room temperature. The ideal chemical formulae is $Na_4[Mg_6Si_4Al_4O_{20}F_4]\bullet H_2O$.

2.2. Synthesis of organo-micas.

The chemical products used for the preparation of the organo-micas were obtained from Aldrich Chemical Co. Neutral amines, hexadecylamine (RNH_2) and dimethylhexadecylamine [$RNH(CH_3)_2$] with R = 16, were firstly converted to the protonated form by adding them to a HCl aqueous solution 0,1 M, in a molar ratio amine:HCl 1:1, and stirred at 80 ºC for 3h. Then, 1 g of Na-4-Mica was added to the protonated amines and left to react for 3h, ~~6h~~ and 24h at 80 ºC. An amount of two-fold excess of the clay CEC of the amines was used in order to favor the cation exchange reaction. For the quaternary amine cations, two-fold excess of the clay CEC of the surfactant cetyltrimethylammonium bromide (CTAB) was dissolved in water and left to react at 80 ºC until equilibrium. The organo-clay was recovered by centrifugation, washed with deionized water and ethanol and dried at room temperature.

2.3. Characterization

XRD. Diffraction patterns were obtained with a Bruker D8 Advance instrument using Cu Kα radiation at 40 kV and 30 mA. The explored angular range was 1.5-70 deg (2θ) at steps of 0.05 deg and a counting time of 5 s/step. Thermogravimetry. TG analysis was performed on a Setaram Setsys evolution TGA-DTA/DSC model coupled at a mass spectrometer Pfeiffer OmniStar. Approximately 20 mg of sample were heated from room temperature to 900 ºC at a heating rate of 10 ºC min^{-1} in air in an open platinum crucible. TEM characterization. TEM images were obtained on a JEOL JEM 2100 microscope with a CeB_6 filament. Samples were prepared by sonication of the powder in ethanol and evaporating one drop onto a holey carbon film. Infrared spectroscopy. Infrared spectra were recorded on a Jasco LE4200 spectrophotometer. The spectra were acquired by accumulation 264 scans at 4 cm^{-1} resolution in the 4000-400 cm^{-1} range. Samples were prepared by mixing the solids with KBr in a 0.5 % proportion.

3. Results and discussion

DSC and TG analyses have been successfully applied to organo-clays for measuring the extension of the cation exchange reaction and hydrophobicity, and for differentiating free and adsorbed organic molecules.[21] Figure 1 includes the TG-DSC curves of untreated mica, and mica in contact with the three cationic surfactants: hexadecylammonium, dimethylhexadecylammonium and trimethylhexadecylammonium. TG curve of the untreated mica exhibits two different regions from the evolution of mass loss with temperature.[22] The first one below 170 ºC corresponds to desorption of water from the clay surface and dehydration of the interlayer sodium. The mass loss of 6.3 % in the first region is related to an endothermic peak

in the DSC diagram. This dehydration process confirms the swelling nature of the synthetic mica. The second mass loss step situated above 600 ºC is associated with clay dehydroxylation. The ~ 1.0 % mass loss observed for the untreated mica in that region of the diagram is probably due to the incomplete fluorination of the terminal oxygen groups in the octahedral layer during the synthesis.

However, up to three steps could be identified in the mass loss curve of the organo-clays, accompanied by a characteristic exothermic or endothermic peak in the DSC curve.[23] A first step in a temperature range from room temperature to 170 ºC (*T_1*) corresponds to desorption of water

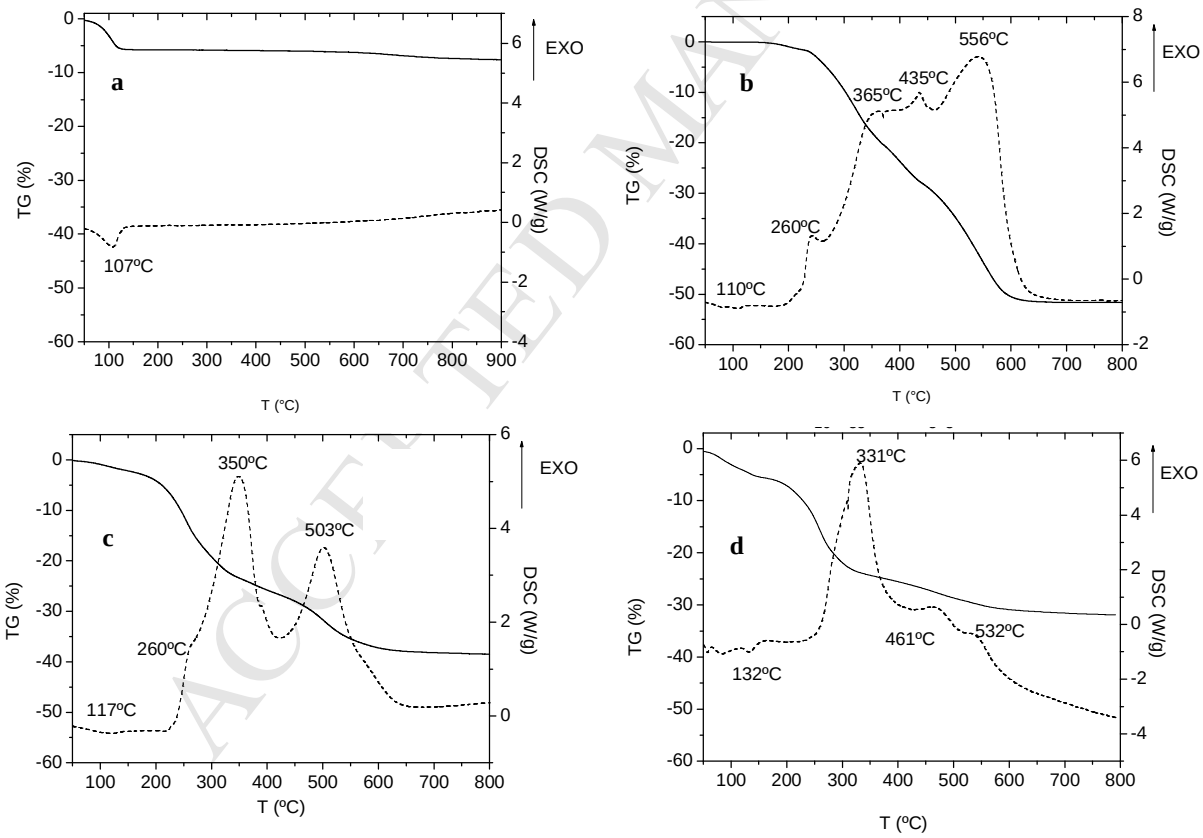

Figure 1. TG (solid line) and DSC (dashed line) plots for Na-4-Mica (a) and for the exchanged products: $C_{16}H_{33}NH_3^+$-Mica -3 hours contact time- (b), $C_{16}H_{33}NH(CH_3)_2^+$-Mica -24 hours

contact time- (c), and $C_{16}H_{33}N(CH_3)_3^+$-Mica -more than 20 days contact time- (d).
from the clay surface and dehydration of the interlayer sodium, both related to an endothermic peak, the shape of DSC curve being independent of the experimental conditions in the first region.

The values of the thermal dehydration are 0.1 %, 2.2 % and 2.7 % in $C_{16}H_{33}NH_3^+$-, $C_{16}H_{33}NH(CH_3)_2^+$- and $C_{16}H_{33}N(CH_3)_3^+$-Mica sample. The adsorbed water in the interlayer space of aluminosilicates is usually associated with inorganic cations, being less probable as the amount of the organics increases due to hydrophobic interactions. So, the amount of desorbed water could be used as an indirect indicator of the extension of the cation exchange reaction and it also provides valuable information about the hydrophilic/hydrophobic nature of the material.

Therefore, the exchanged process with the primary amine cations led to a pure hybrid material with alternating hydrophobic organic and hydrophilic silicate layers. The 0.1 % of hydration could be attributed to the presence of some sodium cations linked to the external surface of the tetrahedral sheet.

However, the water content of the two other samples suggests a partial replacement of the interlayer sodium cations, giving rise to hybrid materials with an interlayer space more hydrophobic when the clay is exchanged with the tertiary amine cations than that obtained when the mica is exchanged with the quaternary amine cations.

A second step, T_2, between 170 ºC and 500 ºC, associated with one or more heat flow peaks, appears as a result of the thermal reactions suffered by the surfactant cations adsorbed onto the mica sample. Characteristic exothermic peaks from the oxidation are showed under air in the DSC curve. Each heat flow is accompanied by its corresponding mass loss step.

Unlike dehydration, the shape of the DSC curve depends on the atmosphere used during the experiment. -Under air atmosphere the organic matter is oxidized to water vapor, CO_2 and NO_2 and the heat flow appears as exothermic peaks-.[23] If the amount of available oxygen is not enough to fully oxidize the organics, the combustion process is prolonged to the next region, and a residue of charcoal is also generated in the reaction. The onset temperature, characteristic of each surfactant, is indicated in figure 1. It has to be mentioned that the evolution of the thermal reactions under air is influenced by the availability of reactive oxygen during the combustion and by the amount of the organics in the bidimensional galleries of mica. Under these particular experimental conditions the oxidation reaction is extended up to the third region of the diagram. In the last step of the thermogram, T_3, situated above 500 ºC, two phenomena could coexist**,** clay dehydroxylation from the clay network and charcoal combustion from the incomplete oxidation of the organic matter in the second region.[24] High charge micas are fluorinated clays, so dehydroxylation is not expected in samples under heating. Depending on the nature of the organic matter, the amount of adsorbed surfactant and oxygen availability, the oxidation process could be extended up to 800 ºC. The area of the exchanged heat peak at those temperatures is directly related to the amount of organics in the interlayer.[25,26] Thus, it can be seen from figure 1 how the area of the curve decreases progressively from $C_{16}H_{33}NH_3^+$-Mica to $C_{16}H_{33}N(CH_3)_3^+$-Mica. TG-DSC measurements were monitored by the evolved gas through mass spectrometry. Data were recorded simultaneously to the TG-DSC analysis helping with the interpretation of the thermal reactions. Figure 2 shows the TG curves including the water and CO_2 evolution during the experiment in air atmosphere of the three organo-micas. Below 500 ºC the mass loss is related to both the elimination of water and CO_2, but only the CO_2 curve is prolonged beyond that temperature. Unlike the other two samples, the maximum in the signal of water curve of the

$C_{16}H_{33}NH_3^+$-Mica only appears in the second region of the diagram. Therefore, there is no adsorbed water associated with this sample, confirming the hydrophobic character of the interlayer and the full exchange of sodium by the surfactant. However, for tertiary and quaternary amine cations, where the exchange reaction was incomplete, the water curve exhibit one peak

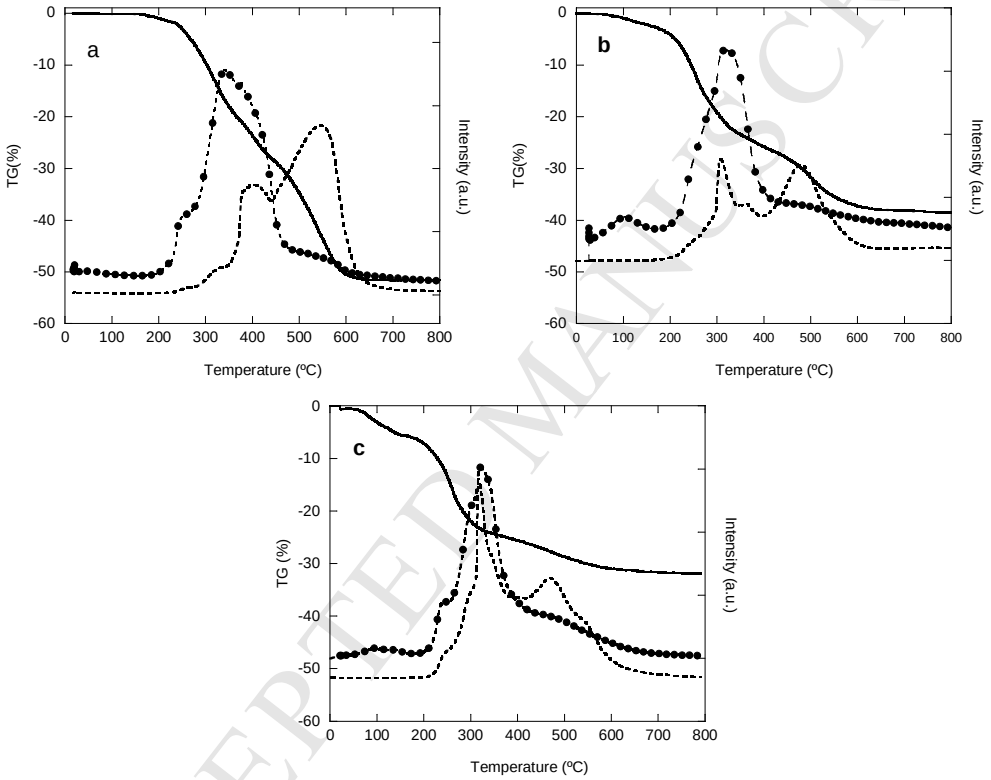

Figure 2. TG (solid line), MS water curve (--●) and MS CO_2 curve (dashed line) for the hybrids: $C_{16}H_{33}NH_3^+$-Mica (a), $C_{16}H_{33}NH(CH_3)_2^+$-Mica (b) and $C_{16}H_{33}N(CH_3)_3^+$-Mica (c).

in the first region, between room temperature and 170 ºC. The combustion of the organic compounds generates several peaks below 500 ºC in the CO_2 and water evolution curves. The residual charcoal from the incomplete combustion of the surfactants is fully oxidized in the third region, above 500 ºC, with a peak in the CO_2 associated with such process.

The extension of the cation exchange, that is, how successful the exchange reaction was, has been determined by TG analysis. Data are included in table 1. The mass loss between room temperature and 170 ºC varies with the surfactant; for the primary amine only 0.12 water molecules per uc of the initial 3.14 molecules remains in the sample, confirming the replacement of Na^+ cations with organic cations in the interlayer space of mica. However, the amount of interlayer water increases for the tertiary amine cation up to 1.61 molecules per uc, and up to 1.84 molecules of water for the cetyltrimethylammonium surfactant cations, indicating that the CECs are not fully satisfied for either of the two last samples. The mass loss in the temperature range 170-800 ºC, corresponding to the removal of the organics, has been used to calculate the number of organic cations in the interlayer after the exchange reaction (also included in table 1).

Table 1. Molecules of water per unit cell and surfactant cations calculated from the TG mass loss curve.

	Molecules H_2O/uc	**Surfactant ions[b]/Si**	**Mass loss step 2 T_2 (170-300 ºC)**	**Mass loss step 3 T_3 (300-800)ºC**
Na-4-Mica	3.14	---	---	---
$C_{16}H_{33}NH_3^+$-Mica	0.12	0.9 (1)[c]	0.32 ions/uc	3.08 ions/uc
$C_{16}H_{33}NH(CH_3)_2^+$-Mica	1.61	0.5 (1)	0.72 ions/uc	1.08 ions/uc
$C_{16}H_{33}N(CH_3)_3^+$-Mica	1.84[a]	0.3 (1)	0.44 ions/uc	0.69 ions/uc

[a] Calculated between 100 and 170 °C. [b] Calculated from the weight loss between 170 and 800 ºC.[c] Theoretical values for the organo-mica in parentheses.

Two features could be described based on the hydrophilicity of the surfactant head: (i) Primary amine cations $[C_{16}H_{33}NH_3]^+$ have almost fully replaced Na^+ cations from the interlayer space of mica, as has been previously proposed in the literature.[17] (ii) The incorporation of methyl groups at the surfactant polar head has two different effects, firstly the size of the head-group increases,

then a greater area of the layer is occupied by the surfactant cations. And secondly the hydrophilicity of the surfactant head decreases, and a softer electrostatic attraction is expected between both, the surfactant cations and the charged clay layer.

Consequently the CEC is not satisfied in $[C_{16}H_{33}NH(CH_3)_2]^+$ and $[C_{16}H_{33}N(CH_3)_3]^+$, with a rate of replacement of ~ 50 % and ~ 40 %, respectively.

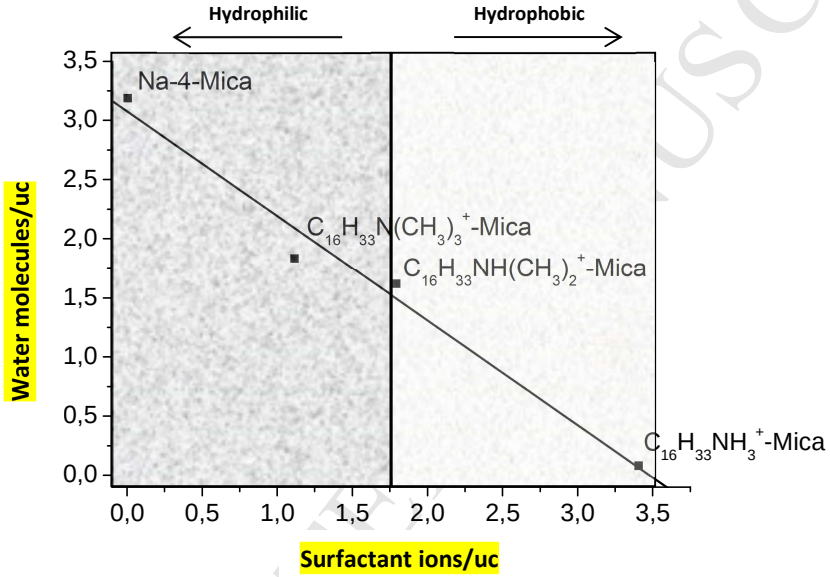

Figure 3. Representation of the hydrophilic/hydrophobic character of the interlayer space of the hybrids.

As result of the treatment different exchanged products have been generated. Figure 3 shows the number of water molecules per uc as a function of the number of surfactant ions per uc. The data included in figure 3 have been calculated from the TG analysis. The plot illustrates the overall hydrophilic/hydrophobic character of the interlayer space, from a fully hydrophilic character at the left region of the plot to a fully hydrophobic character at the opposite right region. Samples with an intermediate character, hydrophilic and hydrophobic, may be positioned in the middle

region. Na-4-Mica and $C_{16}H_{33}NH_3^+$-Mica with an univocal hydrophilic and hydrophobic nature, respectively, are in opposite regions of the plot, whereas an interesting amphiphilic behavior would be extrapolated for the other two samples, $C_{16}H_{33}NH(CH_3)_2^+$-Mica and $C_{16}H_{33}N(CH_3)_3^+$-Mica. However, the occupancy and distribution of the organic/inorganic cations inside the layers is a crucial factor for determining their potential application. When the exchange capacity of the silicate is not fully satisfied several configurations are possible as result of the driving force, attractive electrostatic forces between both cations –organic and inorganic- and the negative charge of the silicate, attractive Van der Waals forces between tails also steric factors are involved. Phase segregation of the organo-clay and the inorganic-clay can occur; an homogeneous single phase of mixed organic and inorganic cations in the interlayer space compensating the layer charge can be formed; or even a heterogeneous phase of alternating organic and inorganic interlayer spaces.

Classically, diffraction techniques have been used for determining the arrangement of alkyl chains on the interlayer of clays based on geometrical considerations. Interlayer cation density and alkyl chain length, together with environmental factors as temperature, are the principal parameters that influence the structure of the organics.[27] Different structures have been proposed based on the basal spacing of high charge micas exchanged with primary alkylammonium cations;

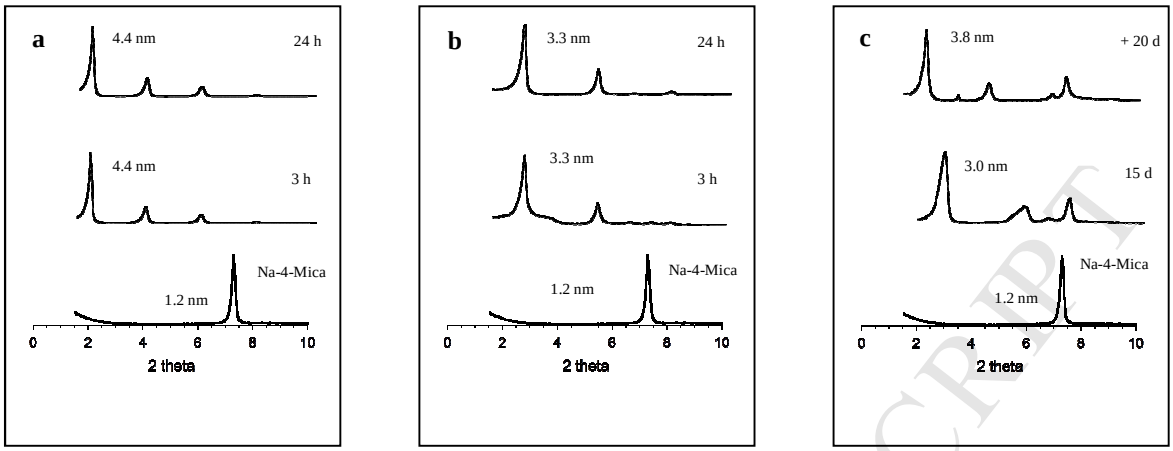

Figure 4. XRD patterns of the exchanged products at different times (a) $C_{16}H_{33}NH_3^+$-Mica, (b) $C_{16}H_{33}NH(CH_3)_2^+$-Mica and (c) $C_{16}H_{33}N(CH_3)_3^+$-Mica.

For short surfactants -below 14 carbon atoms-, the CEC is not satisfied and a mixed structure of monolayer and paraffinic bilayer is found when dodecylammonium is located in the interlayer space of high charge micas with two and three layer charges.[17] In contrast, for the long alkyl chain octadecylammonium the CEC is fully satisfied and a homogeneous bilayer paraffin-like structure has been observed.[18] However, other factors as hydrophilicity and surfactant head group size have not been analyzed in the formation of hybrid materials from high charge micas up to now. XRD patterns of the organo-micas with different reaction times are plotted in figure 4 together with that from the original sample. The strongest peak in the pattern of Na-4-Mica is attributed to the symmetrical basal (001) reflection with a d-spacing value of 1.2 nm. The interlayer composition of this mica has been described as sodium cations accommodated in the ditrigonal holes on the tetrahedral sheet and a pseudo-monolayer of water between the silicate layers. After 3 h of reaction with hexadecylammonium (figure 4a) an increment of the basal space up to 4.4 nm is observed (similar value is obtained after 24 h). Several statements can be

pointed out from the diagram: (1) the initial (001) basal reflection at 7.4º is not present in the pattern. At this stage the sodium cations have been fully replaced by the surfactant hexadecylammonium. This data has been confirmed also from TG experiments. The electrostatic interaction between the polar head and the clay layer, together with the Van der Waals interactions between alkyl groups are strong enough to fully displace sodium cations from the galleries. (2) The XRD patterns exhibit other (00l) basal reflections, indicating a regularly ordered structure and a layer charge homogeneously distributed through the structure.

The different configurations described for alkylammonium cations compensating the CEC of swelling clays, smectites; vermiculites and rare expandable micas correspond to a set of simple geometrical considerations. For example, if the cross-sectional area of the surfactant molecule is greater than the equivalent area, the cation cannot be lying parallel to the clay layer in a monolayer arrangement and adopts a paraffin-type configuration. The equivalent area, A_e, is defined as the layer surface occupied by each monovalent cation, calculated as $a \cdot b/\xi$, where a and b are the cell parameters (0.534 and 0.924 nm, respectively) and ξ is the cationic density in the interlayer based on the TG analysis. The gallery height also gives an idea about the arrangement of the organics inside the interlayer, forming either a monolayer or a bilayer tilted respect to the surface. Table 2 summarizes some geometrical parameters calculated from TG and XRD data. From those data some restrictions can be directly extrapolated.

Firstly, the cationic surfactant hexadecylammonium cannot be lying parallel to the surface because its cross-sectional area is greater than the A_e, even if a parallel bilayer arrangement is considered. Secondly, the high spacing exhibited by this sample is therefore compatible with a paraffin bilayer structure, with the hydrophobic tails pointing toward the interlayer space, tilted 58.2° away from the clay surface.

Table 2. Geometrical parameters and packing properties of the hybrids.

Geometrical parameters	Organic cation in the interlayer		
	$R\text{-}NH_3^+$	$R\text{-}NH(CH_3)_2^+$	$R\text{-}N(CH_3)_3^+$
Cationic density/Si_8O_{20}[a]	3.40	1.80	1.13
Gallery height (nm)[b]	3.46	2.31	2.88
Surfactant head group size ($Å^2$)	15	26	34
Tilting angle,α (°)[c]	58.2	32.2	41.6
A_e monolayer (nm^2)	0.15	0.28	0.44
Cross-sectional area (nm^2)	1.05	1.44	1.68

[a] Calculated from TG; [b]Basal spacing(d_{001}) – 0.94. [c] sinα = gallery height/2lc_{16}

That value is very close to 57.1º, tilting angle reported in the literature.[17] When hexadecylammonium is put in contact with high charge mica a quantitative uptake occurs since the attractive Van der Waals forces between tails of 16 carbon atoms length are strong enough to fully displace sodium cations from exchange sites. In addition, the hydrophilic head group of the surfactant interacts with the surface of the clay gallery through electrostatic forces. Under these conditions, an hydrophobic/hydrophilic hybrid material is generated by alternating hydrophobic galleries fully occupied by surfactant cations and hydrophilic clay layers. Partial substitution of protons by methyl groups in the surfactant head of hexadecylammonium cation increases the hydrophobicity of the polar head group leading in a non-quantitative exchange in high charge mica. Figure 4b shows the XRD patterns after exchanging Na-4-Mica with the surfactant dimetilhexadecylammonium with 3h and 24h contact time. For both reaction times a new family of basal reflections with up to three different spacing could be observed in the diagram, the first peak situated at 2.7º 2θ with a basal space of 3.3 nm. After 24 h of reaction the 1.2 nm reflection characteristic of Na-4-Mica does not appear in the plot, even though the ratio of replacement of

sodium by the surfactant is the 50 % in this sample. Also a paraffin bilayer arrangement of the dimetilhexadecylammonium surfactant on the galleries of the silicate can be extrapolated from data included in table 2. The tilting angle of 32.2 º has been calculated according to the basal space of 3.3 nm and the length of the alkyl chain. To understand the intercalation chemistry of high charge micas when the inorganic cations are partially replaced by organic cations additional considerations have to be taken into account. The relationship between the size of the surfactant head group and the charge density of clay layer has been proposed as a fundamental parameter to determine the exchanged product formation in a fluorohectorite.[13] The charge density can be defined as the area of the clay per one electron charge, and can be calculated as $a \cdot b/q$, where a and b are the cell parameters and q is the deficit of charge per unit cell. Only under the premise that the charge density was large enough to allocate the surfactant head group a homogeneous mixed inorganic-organic intercalated product could be formed. However, for larger head groups, the free space on the clay layer is not enough to allocate both cationic species so the interlayer sodium is displaced from the gallery and a 1:1 organic-Na^+ heterostructure is proposed to be formed. The theoretical high charge Na-4-Mica layer charge density is calculated to be one electron per 15 $Å^2$, however the paraffinic bilayer conformation adopted by the organic into the galleries allows allocating up to two surfactant cations per charge density. Under that assumption there is a surface of 30 $Å^2$ per molecule of surfactant per unit cell. Layer charge density has been calculated from the refined lattice parameters: a = 5.345(1) Å, b = 9.242(1) Å, c = 12.278 (1) Å, β = 98.54(1)° assuming a monoclinic symmetry (S.G. C2/m).[12] The head group size of the three surfactants has been calculated attending to their Van der Waals radii and they are included in table 2. The relationship between the following values, the head group size for dimetilhexadecylammonium and twice the charge density allows the coexistence of sodium and

surfactant in the same gallery. Also the highly hydrophilic clay surface is able to strongly interact with both, solvated sodium and the head of the surfactant so an hydrated homogeneous mixed ion exchange product can be formed. The formation of a heterostructure, with intercalated organic and sodium ions organized in alternating galleries, or in a phase segregation arrangement can be discarded because of the absence of the corresponding Na-4-Mica reflection in the diagram whose associated basal spacing would be ca. 1.2 nm.

Full substitution of hydrogen atoms by methyl in the ammonium head group of hexadecylammonium cation hamper a quantitative uptake of the surfactant. Under that scenario, the weak interaction between the polar head and the highly hydrophilic basal surface of clay leads a rate of replacement of 40 %. Figure 4c includes the XRD patterns of Na-4-Mica after treatment with cetyltrimethylammonium for 15 and more than 20 days. After 20 days three families of reflections have been identified. (1) Fully exchanged organoclay with a basal space of 3.8 nm. The surfactant is accommodated in the galleries in a paraffin-type bilayer conformation, with the polar head matching the surface area of 30 $Å^2$ and the tails pointed out from the surface forming a tilting angle of 41.6º. A (002) reflection could be identified at 4.55º 2θ. (2) The XRD pattern also contains the 1.2 nm reflection characteristic of Na^+ and a pseudomonolayer of water in the interlayer. (3) Finally, two small reflections can be observed in the pattern corresponding to a distance of 2.6 nm and 1.3 nm, respectively, compatible with free cetyltrimethyammonium in the form of bilayer. It has to be mentioned, that two reflections at 4.55º 2θ could coexist, the described second order reflection of the organo-mica and also a pseudo-trimolecular configuration of the surfactant in the interlayer space of mica. This pseudo-trimolecular structure has been previously described for a montmorillonite exchanged with cetyltrimetilammonium when the amount of the surfactant used in the reaction is above 1.9 CEC.[28]

The size of the surfactant head group in the cetyltrimethylammonium cation, slightly higher than 30 Å, and mainly its hydrophobicity precludes the coexistence of the two cationic species in the same interlayer. Water molecules weakly interact with the surfactant and hydrated sodium cations become displaced from the interlayer to the next gallery. Under these equilibrium conditions different exchange**d** products can be formed. Phase segregation can occurs having a mixture of both organic-mica and Na-4-Mica or a rare 1:1 organic:Na^+ heterostructure can be also synthesized. An ordered heterostructure may involve a new reflection in the XRD pattern as result of the sum of the basal spaces of alternating organic and inorganic interlayers, however, no reflection peak is observed in the diagram at that distance.

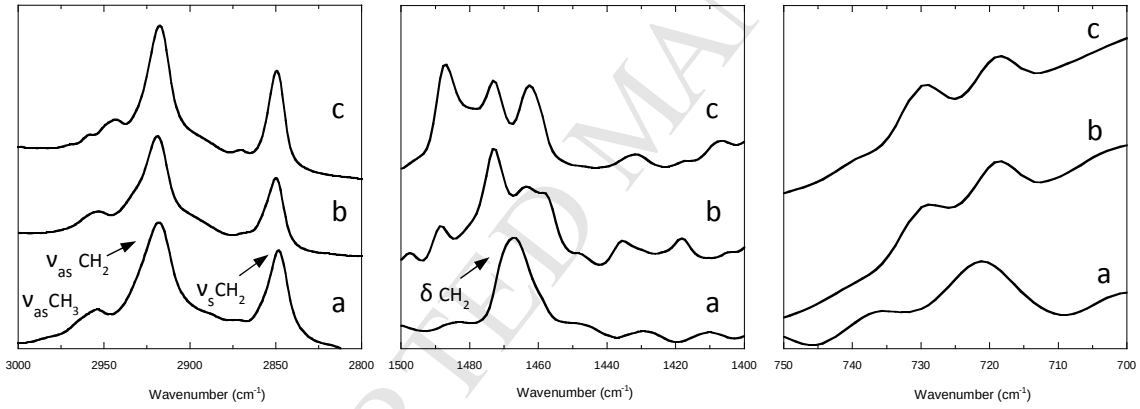

Figure 5. Infrared spectra of the hybrids (a) $C_{16}H_{33}NH_3^+$-Mica -3 hours contact time-, (b) $C_{16}H_{33}NH(CH_3)_2^+$-Mica -24 hours contact time- and (c) $C_{16}H_{33}N(CH_3)_3^+$-Mica –more than 20 days contact time-.

Infrared spectroscopy can provide valuable information about the conformation and packing properties of the methylene chains in an intercalated surfactant bilayer.[29] Figure 5 includes three vibration regions of the FTIR spectra of exchanged samples. In the first region, from 2800 cm^{-1}

to 3000 cm^{-1}, all the samples present the antisymmetric and symmetric $–CH_2$ stretching modes in the spectrum at ~ 2916±1 and 2847±1 cm^{-1} respectively. Only when the surfactant is well packed in the bidimensional gallery of mica, all-trans alkyl chain conformation, $–CH_2$ vibrations are situated in the range 2916-2918 cm^{-1} and 2846-2849 cm^{-1}.[30] For a disorder, liquid-like phase conformation vibrational peaks shift upward, due to the increasing number of gauche conformation alkyl chains, to typical values 2924-2928 cm^{-1} and 2856-2858 cm^{-1}. Also a band due to CH_3 asymmetric stretching is observed in the plot at 2952 cm^{-1}. Not shift of the bands is observed in the spectra as a function of the surfactant head, so it can be said that most of the alkyl chains are in all-trans conformation so there is not enough population in gauche conformation to shift the bands to higher wavenumbers. CH_2 scissoring and rocking modes appear between 1480-1400 cm^{-1} and 750-700 cm^{-1} respectively (second and third region in the plot). Those infrared absorption bands are sensitive to the packing and structure arrangement of the methyl chains.[31] The broad band situated at 1467 cm^{-1} in the spectrum of the sample exchanged with the primary amine is associated to a triclinic, monoclinic or even a hexagonal arrangement of the alkyl chain. In those packing arrangements methylene groups from adjacent chains are weakly interacting. Similar behavior is observed in the CH_2 rocking mode, with a singlet displayed at 720 cm^{-1}. However the singlet splits into two components for the sample exchanged with tertiary and quaternary amines. The vibration bands situated at 1473 cm^{-1} and 1461 cm^{-1} in the CH_2 scissoring mode and at 728 and 718 cm^{-1} in the CH_2 rocking mode, are associated to an orthorhombic cell where surfactant cations are closely packed in the interlayer and methylene groups from adjacent alkyl chains laterally interact. The fact that the alkyl chains of the partially exchanged hybrids strongly interact could be due to an inhomogeneous

distribution of the inorganic cations and the surfactants in the interlayer space of the aluminosilicate.

TEM can be used as a complementary technique to XRD to study the morphology and microstructure of organo-clays, also the photographs can provide a clear idea about the distribution of the organics in the interlayer space of mica.[32] However, the high vacuum of the microscope and the high energy beam can damage the layer structure making the measurements difficult to do. TEM images of the original mica and of the three exchanged samples have been obtained and included in figures from 6 to 9.

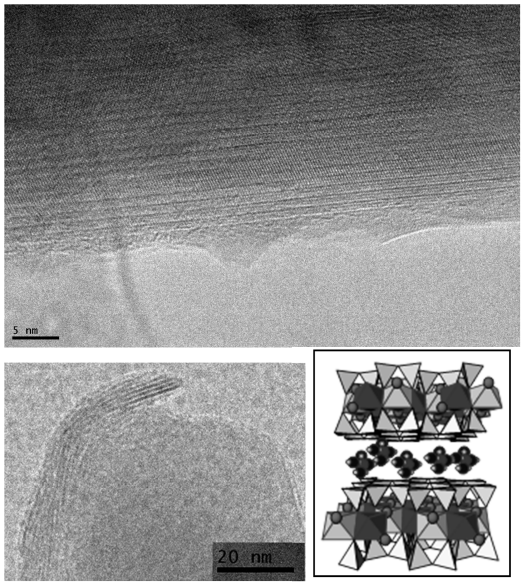

Figure 6. TEM images of the untreated Na-4-Mica.

The layer-structure of the untreated high charge mica can be clearly identified from the image, with a regular basal space of around 1.1 nm -in agreement with the XRD result-, indicating a well ordered structure. The measured basal space confirms that water is still adsorbed onto the interlayer sodium, even under the high energy beam used in the experimental condition where

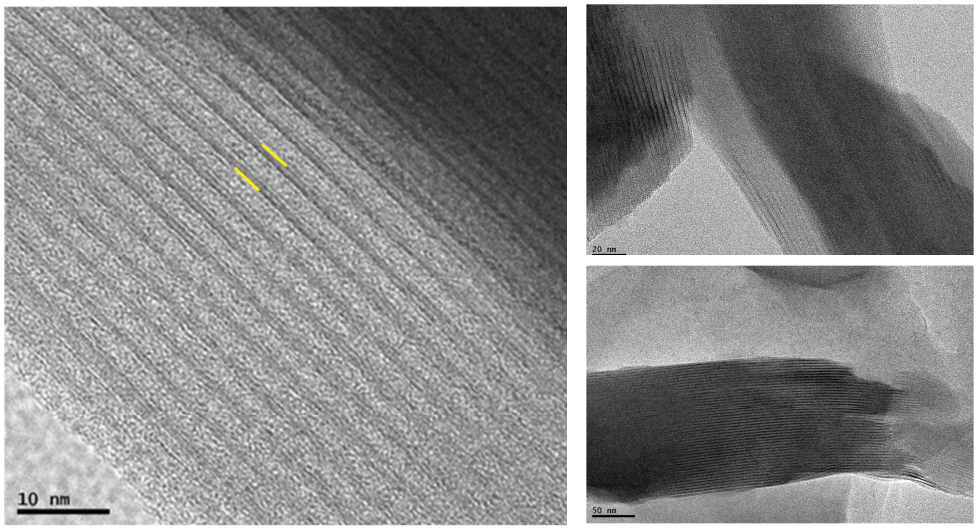

Figure 7. Representative TEM images of the fully exchanged $C_{16}H_{33}NH_3^+$-Mica.

dehydration can occur. Figure 6 also shows a representative image of the sample morphology, where some curved layers can be identified as it has been previously described for a Na or Ca-montmorillonite.[33] Figure 7 shows the micrographs of the sample exchanged with the primary amine surfactant cations. The organo-mica is almost composed of regularly interlayer layers as result of the higher packing density of surfactant inside the galleries. This fact is also corroborated by the number of harmonics exhibited by the XRD diagram. However, slight differences in the basal distance can be observed in the same interlayer along the particle and between neighboring interlayer spaces in the same particle with an average basal space of 4.0 nm, close to the 4.4 nm calculated from the XRD technique. This sample treated with the surfactant also exhibits some changes in the morphology compared to the original mica, also described for other organic clays. The high loading of surfactant between the layers transforms the flexible curved layers described in figure 6 into more rigid flat plates as can be observed from the images in figure 7. Representative micrographs of the partially exchanged sample

$C_{16}H_{33}NH(CH_3)_2^+$-Mica are included in figure 8. A regularly intercalated layer phase could be extrapolated from the images. Compared to the previous sample much more differences in the basal distance could be observed for the neighbor's layers in the particle and even for the same interlayer, with spacing values between 2.4 and 3.0 nm, probably due to an inhomogeneous distribution of the inorganic cation and the surfactant inside the interlayer as has been previously proposed from the infrared measurement. Also, looking at the particle morphology few curved layers similar to the untreated mica could be also identified, mostly at the edges. However, most layers are flat plates although the lower content of surfactant compared to the sample exchanged with the primary amine cations.

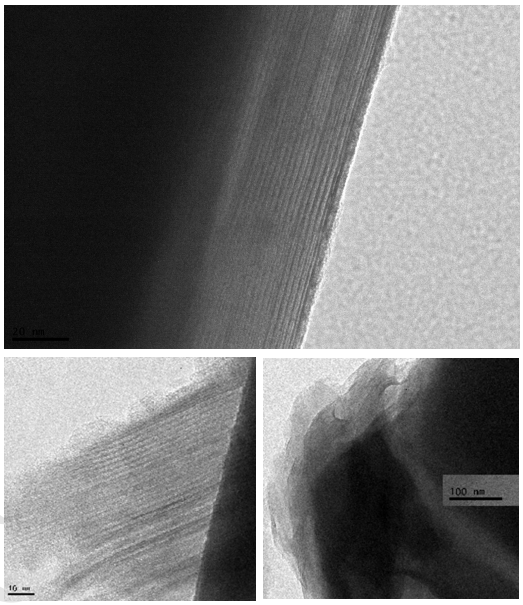

Figure 8. Representative TEM images of the sample $C_{16}H_{33}NH(CH_3)_2^+$-Mica.

In figure 9 representative micrographs of the sample partially exchanged with the quaternary amine cations are included. TEM measurements provide clear information about the distribution of the surfactant in the structure of mica from which a mixture of phases could be identified.

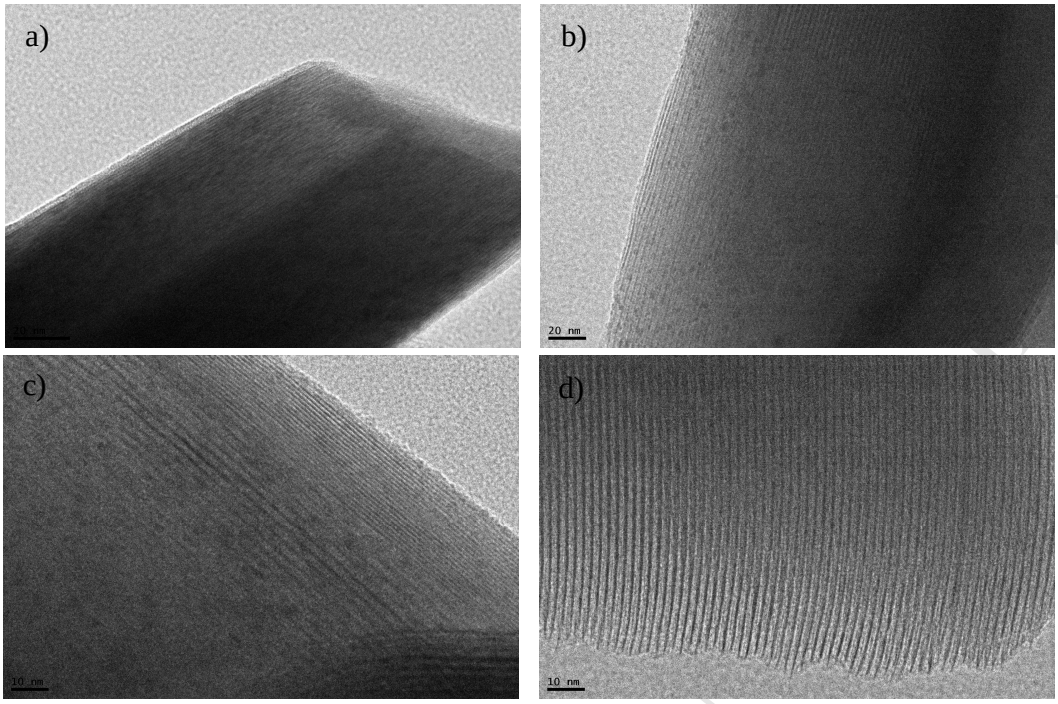

Figure 9. Representative TEM images of the sample $C_{16}H_{33}N(CH_3)_3^+$-Mica.

Phase segregation of the inorganic-clay and organo-clay can be deduced from (a) and (b) pictures. The calculated interlayer of ~1.1 nm (figure 9a) indicates that sodium is still in the interlayer space of some mica particles in which the exchange reaction has not been taken place. Also, clay particles with a fully hydrophobic interlayer space could be identified (figure 9b) with a basal space approximately of 3.6 nm. Those observations are in agreement with the XRD results where characteristic reflections of both kinds of layer families are present in the diffractogram. Also, infrared measurements indicates a close packing conformation of the alkyl chains in the interlayer, compatible with the presence of some pure organo-clay phase in the sample. Other distribution of the organic and inorganic cations in the sample can be deduced from figure 9c, where a heterogeneous phase of organic galleries and inorganic galleries is formed in the same particle. Figure 9d exhibits the image of an organo-clay with a shorter basal space (2.2 nm) confirming the pseudo-trimolecular conformation proposed from the XRD analysis.

4. Conclusions

High charge mica with four layer charges has been exchanged with a primary $(RNH_3)^+$, tertiary $[RNH(CH_3)_2]^+$ and quaternary amine $[RN(CH_3)_3]^+$, with alkyl length R = 16. A combination of X-ray diffraction, thermogravimetric analysis, Fourier transform infrared spectroscopy and transmission electron microscopy techniques have provided a deep insight into the configuration and distribution of the organic/inorganic interlayer of the exchanged-products. The role of the surfactant head groups on the formation of the heteroionic structures when the exchange capacity is not fully satisfied has been also determined. In the present study a correlation between coverage and intercalation properties of high charge micas has been stablished in terms of layer charge and surfactants nature. Particularly the size (steric effects) and the hydrophobic/hydrophilic character of the surfactant head group play a fundamental role in defining the composition of the exchanged-product. A fully hydrophobic interlayer is obtained when the primary amine is intercalated in the mica. However, an hydrated homogeneous mixed inorganic-organic cation in the interlayer of the exchanged product is observed when the tertiary amine is used. Mixed ion clays that combine both exchangeable inorganic and organic ions in their interlayer space can be potential material to be used as adsorbents for water decontamination, independently of the hydrophilic or hydrophobic nature of the pollutants. For the quaternary amine steric effects preclude the coexistence of both organic and inorganic species in the same interlayer of the clay, so phase segregation and an heterostructure configuration are identified as the exchanged products. Thus, a tunable hydrophobicity in the interlayer space of the hybrid material can be obtained under particular experimental condition, from a fully hydrophobic medium to an amphiphilic quasi-solution, needed for a variety of application.

AUTHOR INFORMATION

Corresponding Author

* Departamento de Química e Ingenieria de Procesos y Recursos, Escuela Técnica Superior de Ingenieros Industriales y de Telecomunicación, Universidad de Cantabria, Avda. de Los Castros s/n, 39005, Santander, Spain.

perdigonac@unican.es

Tel:+34 942201592

Author Contributions

The manuscript was written through contributions of all authors. All authors have given approval to the final version of the manuscript.

Funding Sources

Funding from the Ministerio de Economía y Competitividad, under project MAT2015-63929-R is also acknowledge.

ACKNOWLEDGMENT

We would like to thank SERMET from University of Cantabria for providing access to the microscope facility.

ABBREVIATIONS

TGA, termogravimetric analysis; DSC, differential scanning calorimetry ; XRD, x-ray Diffraction; FTIR, fourier transform infrared spectroscopy; TEM, trasnmission electron microscopy.

SYNOPSIS (Word Style “SN_Synopsis_TOC”). If you are submitting your paper to a journal that requires a synopsis, see the journal’s Instructions for Authors for details.

(1) M. Gregorkiewitz, J.A. Rausell-Colom, Amer. Mineral. 72 (1987) 515.

(2) T. Kodama, S. Komarneni, J. Mater. Chem. 9 *(*1999) 533.

(3) T. Kodama, S. Komarneni, W. Hoffbauer, H. Schneider, J. Mater. Chem. 10 (2000) 1649.

(4) T. Kodama, Y. Harada, M. Ueda, K. Shimizu, K. Shuto, S. Komarneni, Langmuir 17 (2001) 4881.

(5) R. Ravella, S. Komarneni, C. Enid-Martínez, Environ. Sci. Technol. 42 (2008) 113.

(6) M.D. Alba, M.A. Castro, M. Naranjo, E. Pavón, Chem. Mater. 18 (2006) 2867.

(7) R. Ravella, S. Komarneni, App. Clay Sci. 39 (2008) 185.

(8) S. Komarneni, R. Pidugu, J.E. Amonette, J. Mater. Chem. 8 (1998) 208.

(9) A. Galarneau, A. Barodawalla, T.J. Pinnavaia, Nature 374 (1995) 531.

(10) Y. Xi, R.L. Frost, H. He, T. Kloprogge, T. Bostrom, Langmuir 21 (2005) 8675.

(11) G. Lagaly, Solid State Ionics 22 (1986) 43.

(12) A.C. Perdigón, D. Li, C. Pesquera, F. González, B. Ortiz, F. Aguado, C. Blanco, J. Mater. Chem. A 1 (2013) 1213.

(13) W.L. Ijdo, T.J. Pinnavaia, J. Sol. St. Chem. 139 (1998) 281.

(14) B. Klebow, A. Meleshyn, Langmuir 28 (2012) 13274.

(15) Z. Klapyta, T. Fujita, N. Iyi, Appl. Clay Sci. 19 (2001) 5.

(16) W.L. Ijdo, T. Lee, T.J. Pinnavaia, Adv. Matt. 8 (1996) 79.

(17) M.D. Alba, M.A. Castro, M.M. Orta, E. Pavón, M.C. Pazos, J.S. Valencia Rios, Langmuir 27 (2011) 9711.

(18) M.C. Pazos, M.A. Castro, M.M. Orta, E. Pavón, J.S. Valencia-Rios, M.D. Alba, Langmuir 28 (2012) 7325.

(19) M.C. Pazos, A. Cota, F.J. Osuna, E. Pavón, M.D. Alba, Langmuir 31 (2015) 4394.

(20) M. Park, D.H. Lee, C.L. Choi, S.S. Kim, K.S. Kim, J. Choi, Chem. Mater. 14 (2002) 2582.

(21) S. Yariv, App. Clay Sci. 24 (2004) 225.

(22) I. Lapides, M. Borisover, S. Yariv, J. Therm. Anal. Calorim. 105 (2011) 921.

(23) Z. Li, W. T. Jiang, H. Hong, Spectrochim. Acta Part A 71 (2008) 1525.

(24) S. Yariv, M. Borisover, J. Therm. Anal. Calorim. 105 (2011) 897.

(25) X. Xi, W. Martens, H. He, R.L. Frost, J. Therm. Anal. Calorim. 81 (2005) 91.

(26) L. Zhaohui, J. Wei-The, Thermochim. Acta 483 (2009) 58.

(27) G. Lagaly, Clay Minerals 16 (1981) 1.

(28) Y. Xi, Z. Ding, H. He, R.L. Frost, J. Colloid Interf. Sci. 277 (2004) 116.

(29) N.V. Venkataraman, S. Vasudevan, J. Phys. Chem. B 105 (2001) 1805.

(30) Y. Li, H. Ishida, Langmuir 19 (2003) 2479.

(31) M. Yuehong, Z. Jianxi, H. Hongping, Y. Peng, S. Wei, Spectrochim. Acta Part A 76 (2010) 122.

(32) H. He, R. Frost, T. Bostrom, P. Yuan, L. Duong, P. Yang, L. Duong, D. Yang, Y. Xi, J.T. Kloprogge, App. Clay Sci. 31 (2006) 262.

(33) B. Bauluz, D.R. Peacor, R.F. Ylagan, Clays Clay Miner. 50 (2002) 157.

Highlights

1. A study of the structural and intercalation properties of a swellable high charge mica exchanged with long alkylammonium cations at different coverages.
2. A tunable hydrophobicity, from a fully hydrophobic interlayer space to an amphiphilic quasi-solution, can be obtained under particular experimental conditions.
3. A correlation between coverage and intercalation properties of high charge micas has been stablished in terms of layer charge and the surfactants nature.